JOURNAL OF PROPULSION AND POWER
Vol. 22, No. 2, March–April 2006

Technical Note

TECHNICAL NOTES are short manuscripts describing new developments or important results of a preliminary nature. These Notes should not exceed 2500 words (where a figure or table counts as 200 words). Following informal review by the Editors, they may be published within a few months of the date of receipt. Style requirements are the same as for regular contributions (see inside back cover).

Strut-Based Gaseous Injection into a Supersonic Stream

S. L. N. Desikan* and Job Kurian†
Indian Institute of Technology Madras, Madras 600 036, India

Introduction

MIXING of a secondary jet with the primary supersonic stream is of great importance in many practical applications especially in scramjet combustors. Because the residence time of the high-speed flow in such combustors is only a few milliseconds, it is essential to implement mixing augmentation techniques to provide rapid and uniform mixing of fuel and air. Several injection schemes have been proposed,[1–5] and it has been concluded that the vorticity is the main driving mechanism for rapid near-field mixing. The present study is conducted on the strut-based fuel injectors. The main advantage of strut-based injectors is the injection of the fuel into the core of the main flow and uniform spreading of the fuel in the lateral direction. The large-scale structures at the wake region can assist macromixing. Moreover, the shock that emanates from the leading edge of the strut is useful to enhance the mixing via the baroclinic torque mechanism.[6] A further advantage of strut-based injection is the formation of a recirculation zone, which can be used for flame holding in combustion.[7–9] Four types of fuel injectors are considered in the current experimental investigation, one of them being the plain strut-type injector. Diagnostic methods employed are Mie scattering combined with image processing and the time-averaged schlieren. Numerical simulation of the flowfield using the commercially available software FLUENT has also been carried out.

Experimental Setup

The facility used for the present study is the blowdown supersonic freejet facility of Mach number 1.7. A test section of width 20 mm, height H 80 mm, and length 300 mm accommodates the injector model. The injector is kept at a distance 40 mm from the inlet to the test section and spans its full width. The secondary air is injected parallel to the mainstream through two 3.4-mm-diam ports. The ports are at a distance of 7 mm from the side walls in the base of the strut. The injection pressure was maintained in such a way that the flow is sonic at the injection ports. The injectant jet was always maintained underexpanded.

Received 23 March 2005; accepted for publication 22 September 2005.

*Research Scholar, Gas Dynamics Laboratory, Department of Aerospace Engineering, Chennai; desikan_sln@yahoo.com.

†Professor, Department of Aerospace engineering, Chennai; kurian@ae.iitm.ac.in.

Injector Configurations

Figure 1 shows the proposed injector models. All of the injectors have length of 96.9 mm, width 20 mm, thickness 6 mm, and wedge angle of 8 deg. C1 is the plain strut injector and C2 the strut with raised and relieved straight ramps at the trailing edge. In the case of injector with ramp, it is well known that the vorticity will be generated due to the spillage of air from the high-pressure ramp surface to the low-pressure adjacent region. Because the adjacent surfaces are the expansion regions (relieved), it is expected that the strength of the vorticity becomes more dominant as compared to the straight adjacent surfaces. Injectors C3 and C4 are the straight castellated and tapered castellated-type strut injectors.

In the case of injector C3, there is a projected and recess region of 10 mm in the aft portion of the strut, whereas in injector C4, the projected portion is uniformly tapered by 2 deg. It is expected that the flow over the projected surface will enter into the expanded low-pressure recess region due to the pressure difference and produce vorticity. This would enhance the mixing, and the effectiveness is expected to be greater if the projected region is tapered. In these cases it is attempted to enhance mixing due to vorticity without the shocks of the ramp injectors. While designing the injectors, care is taken to keep the blockage below 10%. The raised ramp angle of 14 deg is chosen, to keep the blockage within the preceding limit. The relieved ramp angle of 5.7 deg is chosen so that the base of the injector C2 is 4 mm thick, which can accommodate the injection port of 3.4 mm diam. To accommodate the injector port of 3.4 mm diam, the maximum possible taper that can be given to injector C4 is 2 deg.

Diagnostic Methods

A continuous-wave, 15-mW He–Ne laser source was used as the light source in the experiments. For the planar Mie-scattering experiments, a laser sheet of about 1 mm thickness was formed from the laser source. The injectant air was seeded with olive oil. Mie images were captured using a charge-coupled device (CCD) camera (Stanford Computer Optics, Inc., Model MV10-OEM). The images were acquired at a 55-deg angle to the longitudinal axis of the test section at nine cross-sectional locations X downstream of the injection ports. The location closest to the injection port was at $X/t = 0.83$, where t is the thickness of the strut. The camera shutter speed corresponds to an exposure time of 56.8 ms. The acquired images were processed using an in-house developed software. The software implements background subtraction and flat-field correction to eliminate unwanted noise, nonuniformity of the laser light sheet, and thermodynamic dependency of the flowfield.[10] A parameter, degree of unmixedness (DU),[11,12] is used to compare the mixing capability of the injection schemes employed. DU is defined as the ratio of the standard deviation of the pixel intensities of the image to the average of the image pixel intensities. The statistical calculation was performed on the entire image field, and the value of DU was calculated based on the average intensities of six images at each location. Based on the accuracy of the instrumentation and the method of image processing, the uncertainty in the estimation DU is ±7%.

Results and Discussion

Figure 2 shows the schlieren images of the flow without (Fig. 2a) and with (Fig. 2b) injection. The injector positions are visible on

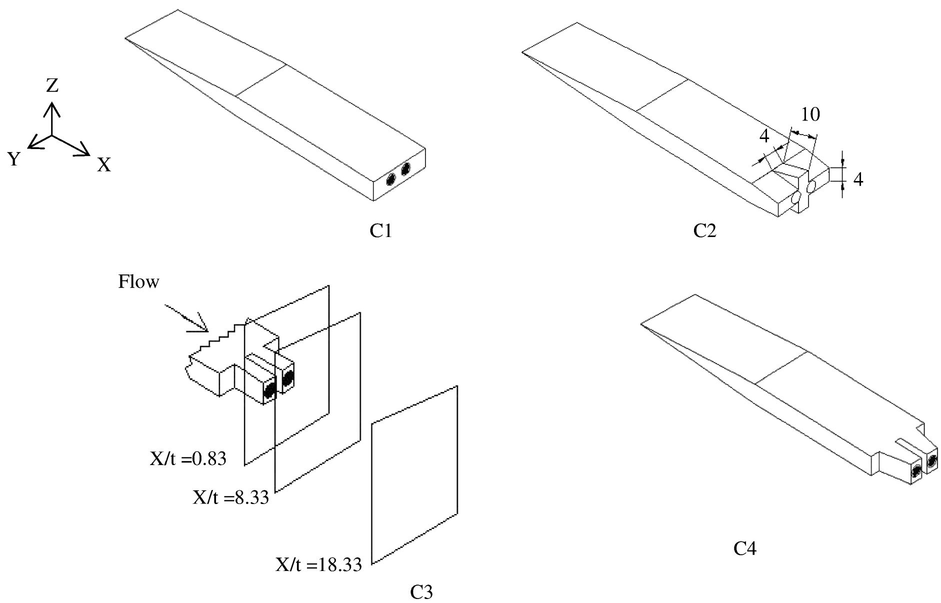

Fig. 1 Injector configurations, dimensions in millimeters.

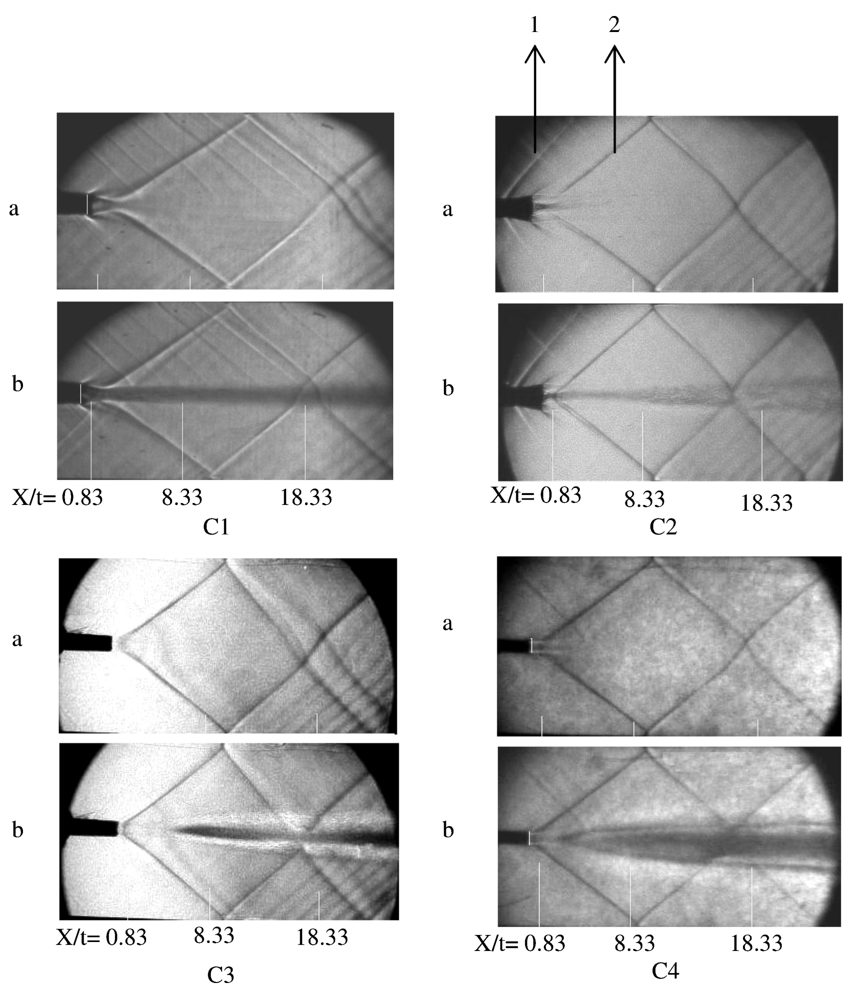

Fig. 2 Schlieren images behind the strut without and with injection: 1 ramp shocks and 2, recompression shocks.

the left of the image, and the flow is from left to right. Each image extends to about 150 mm from the base of the strut. The general features of the flowfield show the expansion around the strut base and the formation of recompression shocks. The main flow, which is separated by the presence of strut, reattaches downstream of the strut base and causes the formation of recompression shocks. The recompression shocks make the flow parallel to the freestream. The change in density near the base region of the strut observed from the schlieren images confirms the existence of the recirculation region in the vicinity of the recompression shocks. The recirculation entrains the jet and causes it to spread over the entire base region. However the point where the recompression shocks originate is the wake neck. Note that, in all of the injection images, the injectant narrows as it passes through the wake neck before spreading again. Moreover, it is seen that, the location of the wake neck changes with the injector geometry. In the case of injectors C1 and C3, it

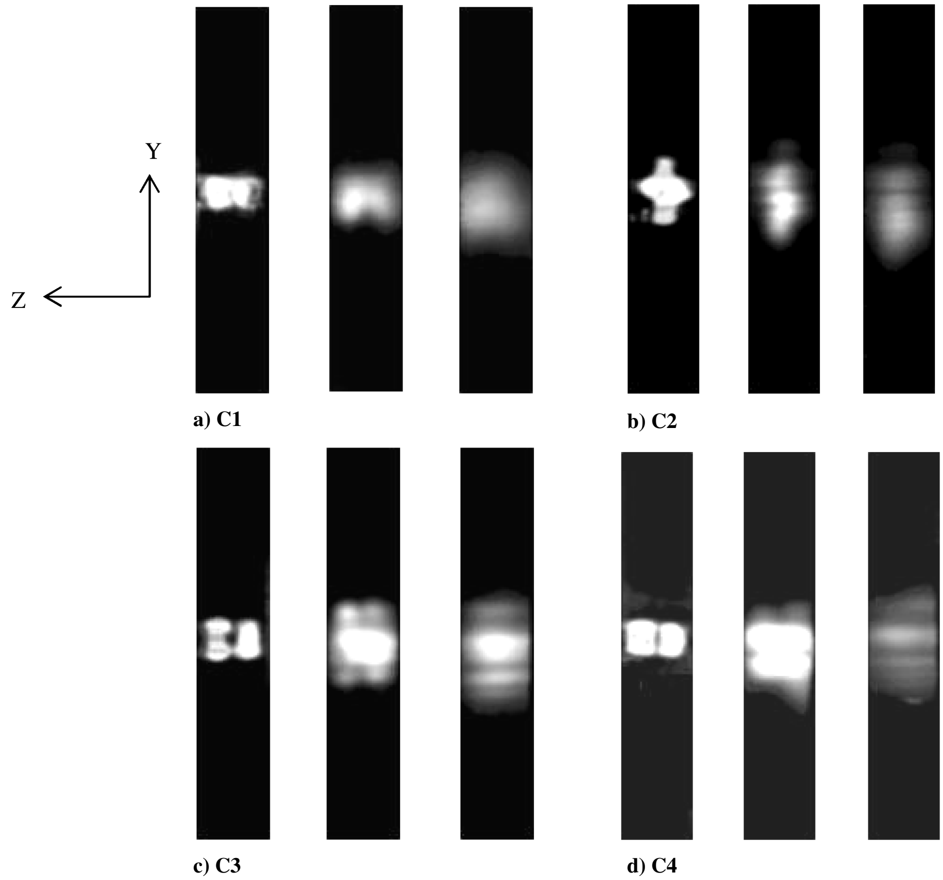

Fig. 3 Mie images at various *X/t*: left, 0.83; center, 8.33; and right, 18.33.

is observed that the intersection point of the recompression shock is slightly shifted from the centerline of the test section. This may be due to unsteady nature of the shock pattern, which could not be diagnosed in the time-averaged schlieren pictures. While designing C2 injector, it was expected that the shock produced by the raised ramp would intersect with the injectant plume and enhance the mixing due to the baroclinic torque mechanism. However, the schlieren images of injector C2 shows that the ramp-generated shocks are not strong enough to reflect back from the wall of the test section into the injectant plume. The injected jet is highly underexpanded, and as it passes through the surrounding medium of lower pressure, it will form a three-dimensional barrel shock and the Mach disk. In the present case, the schlieren images show no evidence of such effects. The injection is done behind the strut where the subsonic recirculation exists; the interaction between the underexpanded jet and the surrounding subsonic recirculating region is seen to be masked in the schlieren pictures. It is further found that the C4 injector exhibits good spreading as compared to the other injectors.

In the present study, the Reynolds number based on the strut length is calculated as 8.26×10^6 and the maximum boundary layer thickness is 1.48 mm. As far as the strut injector is concerned, the nature of the boundary layer and its associated phenomena are important with regard to the total pressure losses. If the boundary layer is separated in the region close to the leading edge, the total pressure loss will be greater. Earlier works on strut injectors[13,14] suggested that the strut of semiwedge angle of 6 deg and the leading-edge radius of 1 mm does not produce a separation bubble in Mach 2.5 flow. In the present case, the semiwedge angle is only 4 deg and the leading edge is of zero thickness. Hence, it is expected that flow separation will not occur for the present case. Based on this, it is reasonable to presume that the chosen length and height of the strut have only a minor influence on the loss in total pressure.

To assess the mixing of the injectant with the main flow, cross-plane imaging at nine different locations were carried out using a planar Mie-scattering technique. Figure 3 shows the Mie images at three selected locations, namely, $X/t = 0.83$, 8.33, and 18.33. Here X is the distance downstream of the injection location and is nondimensionalized by t, the thickness of the strut. Figure 3a corresponding to injector C1, shows that the spreading of the injectant plume is very minimum.

Figure 3b, corresponding to injector C2, shows the stretching of the jet plume in the vertical direction. This could be attributed to the vorticity formation from raised and relieved ramps. Also note that the spreading of the jet is not very pronounced in the crosswise direction. The vorticity generated by the ramps on either side of the strut stretches the injectant in the vertical direction rather than over the complete base of the strut. In the Figs. 3c and 3d corresponding to injectors C3 and C4, better spread of the injectant in the lateral, as well as in the crosswise, direction is observed. Of these two, the spreading is found to be marginally better in the latter case. This could be attributed to the increased vorticity strength produced by the tapered castellated portion.

The numerical simulation of the flow was also carried out using FLUENT for the straight castellated strut (injector C3) and for the tapered castellated strut (injector C4) to show the generated velocity vector field in the castellated region. The flowfield is three-dimensional and is fully compressible. Turbulence is modeled using a $k{-}\omega$ model with standard wall functions. All solid surfaces have been taken to be adiabatic, no-slip surfaces. Pressure inlet and mass flow inlet boundary conditions are used for the duct inlet and injection inlet, respectively. Default values of k and ω have been used for the inflow. At the outflow boundary, all of the variables are calculated by extrapolation from the interior. The computational domain consisted of approximately 370,000 tetrahedral cells, and finer meshes are used in the regions where shocks are seen. The wall y^+ was found to be 200–250 in all three injector cases. The mass flux residuals in all cases are of the order of 10^{-5}. A grid-independence study has been carried out for the injectors. Adoption based on the gradient of static pressure has been used in this numerical work.

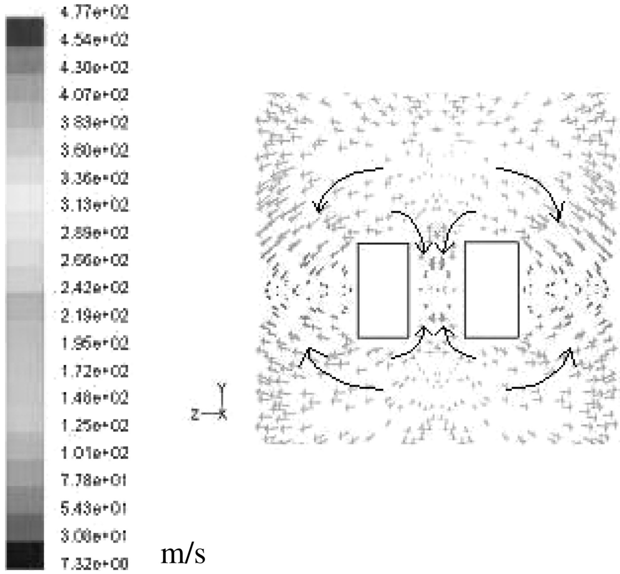

Fig. 4 Velocity vector in castellated region.

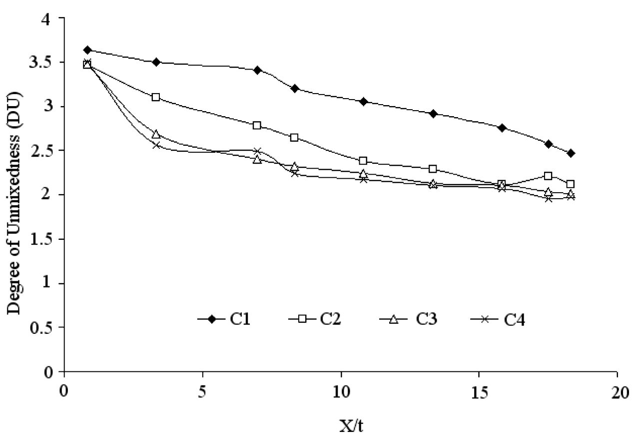

Fig. 5 DU variation for different *X/t* locations.

Figure 4 shows the simulated velocity vector in the castellated region. Figure 4 corresponds to the section at 96 mm from the leading edge of the strut (injector C3) in the y–z plane, which gives evidence of the vorticity generation in the castellated portion of the flowfield. The directions of the velocity vector turning around the castellated region are shown in Fig. 4. When the castellated portion of the strut is tapered, the resulting pressure variation in that region can enhance the strength of the vorticity generated by it and, hence, enhance mixing. In the case of injector C4, the generated velocity vector varies up to 600 m/s, whereas in the case of injectors C2 and C3, the velocity vector has a maximum of 477 m/s. This is consistent with the increased mixing observed while using injector C4 as shown in Figs. 3d and 5. Figure 5 shows DU vs X/t. Note that the value of DU drops initially, except for injector C1. This could be attributed to the effect of vorticity. From the experimental results, it is not presumptuous to consider that the change of slope of the DU curve is an indication of the mode of mixing. Earlier work[15] on ramp-based injector indicates that the vorticity generated is effective for mixing up to a distance of 10 times the ramp height. The change of slope of the DU curve in the case of injector C2 is occurring at a similar location, namely, $\sim X/t = 6$. In the case of injectors C3 and C4, it occurs at approximately four times the height of the strut base. From the Mie images, it is found that stripes of horizontal lines are visible at $X/t = 18.33$. This location is very close to the intersection point of the reflected shocks (Fig. 2b). This could be the reason for the occurrence of the horizontal lines in the Mie images. Kinks seen in the DU curves are roughly within the uncertainty limits. The taper given for the castellated portion is small in the case of injector C4; its performance is seen to be not different from that of injector C3. The performance of the ramp-strut (injector C2) injector falls in between that of the plain strut and of the castellated-type injectors.

Conclusions

Schlieren photography and the Mie scattering technique were employed to study the flowfield of the injectant plume produced by four strut-based injectors. The results were compared with that of the plain strut injector. The performance of the injectors as regards mixing is compared using the DU parameter. It has been found that the castellated injectors (injectors C3 and C4) performed better compared to other two cases. The ramp-strut injector (injector C2) performed better compared to the plain strut injector (injector C1). The flowfield simulated using FLUENT explains the better performance of the castellated injectors to some extent.

References

[1]Donohue, J. M., Haj-Hariri, H., and McDaniel, J. C., "Vorticity Generation Mechanisms in Parallel Injection Schemes for Supersonic Mixing," AIAA Paper 92-3286, July 1992.

[2]Waitz, I. A., Marble, F. E., and Zukoski, E. E., "Investigation of a Contoured Wall Injector for Hypervelocity Mixing Augmentation," *AIAA Journal*, Vol. 31, No. 6, 1993, pp. 1014–1021.

[3]Stouffer, S. D., "Effects of Compression and Expansion Ramp Fuel Injector Configurations on Scramjet Combustion and Hear Transfer," AIAA Paper 93-0609, Jan. 1993.

[4]Hartfield, R. J., Hollo, S. D., and McDaniel, J. C., "Experimental Investigation of a Supersonic Swept Ramp Injector Using Laser-Iodine Fluorescence," *Journal of Propulsion and Power*, Vol. 10, No. 1, 1994, pp. 129–135.

[5]Donohue, J. M., McDaniel, J. C., and Haj-Hariri, H., "Experimental and Numerical Study of Swept Ramp Injection into a Supersonic Flowfield," *AIAA Journal*, Vol. 32, No. 9, 1994, pp. 1860–1867.

[6]Marble, F. E., Hendricks, G. J., and Zukoski, E. E., "Progress Toward Shock Enhancement of Supersonic Combustion Process," AIAA Paper 87-1880, June 1987.

[7]Fox, J. S., Gaston, M. J., Houwing, A. F. P., and Danehy, P. M., "Comparison of Hypermixing Injectors Using a Mixture-Fraction-Sensitive Imaging Technique," *13th Australasian Fluid Mechanics Conference*, 13–18 Dec. 1998, pp. 79–82.

[8]Kodera, M., Sunami, T., and Scheel, F., "Numerical Study of the Supersonic Mixing Enhancement Using Streamwise Vortices," AIAA Paper 2002-5117, Oct. 2002.

[9]Gerlinger, P., and Brijggemann, D., "Numerical Investigation of Hydrogen Strut Injection into Supersonic Airflows," *Journal of Propulsion and Power*, Vol. 16, No. 1, 2000, p. 22–28.

[10]Hartfield, R. J., Hollo, S. D., and Daniel, J. C., "Experimental Investigation of a Supersonic Swept Ramp Injector Using Laser-Induced Iodine Fluorescence," *Journal of Propulsion and Power*, Vol. 10, No. 1, 1994, pp. 129–135.

[11]Liscinsky, D. S., True, B., and Holdeman, J. D., "Mixing Characteristics of Directly Opposed Rows of Jets Injected Normal to a Cross Flow in a Rectangular Duct," AIAA Paper 94-0217, Jan. 1994.

[12]Kurian, J., and Subash, S., "Studies on Gaseous Injection into Supersonic Free Stream," *16th International Symposium on Airbreathing Engines*, Paper 2003-1175, Aug. 2003.

[13]Masuya, G., Komuro, T., Murakami, A., Murayama, M., and Ohwaki, K., "Ignition and Combustion Performance of Scramjet Combustors with Fuel Injection Struts," *Journal of Propulsion and Power*, Vol. 11, No. 2, 1995, pp. 301–307.

[14]Gerlinger, P., and Bruggemann, D., "Numerical Investigation of Hydrogen Strut Injections into Supersonic Airflows," *Journal of Propulsion and Power*, Vol. 16, No. 1, 2000, pp. 22–28.

[15]Hartifield, R. H., Jr., Hollo, S. D., and McDaniel, J. C., "Experimental Investigation of a Supersonic Swept Ramp Injector Using Laser-Induced Iodine Fluorescence," *Journal of Propulsion and Power*, Vol. 10, No. 1, 1994, pp. 129–135.